

RADIOTHERAPY TREATMENT PLANNING BY ADJOINT AND FORWARD TRANSPORT AND ANALYSIS

Michael E. Kowalok, Robert Jeraj, Tim D. Bohm, and T. Rock Mackie

Department of Medical Physics, University of Wisconsin - Madison

1530 MSC, 1300 University Ave, Madison, WI 53706

mkowalok@wisc.edu; rjeraj@wisc.edu, tdbohm@wisc.edu, trmackie@wisc.edu

Douglass L. Henderson

Department of Engineering Physics, University of Wisconsin - Madison

153 ERB, 1500 Engineering Dr, Madison, WI 53706

henserson@engr.wisc.edu

ABSTRACT

We report on an iterative scheme of adjoint and forward Monte Carlo transport calculations that automatically selects beam weights for IMRT. The iterative scheme begins with an adjoint calculation for each target and sensitive structure ROI. These calculations provide an estimate of which source positions and directions are most important for treating the target ROI while avoiding sensitive structure ROIs. These adjoint tallies are combined into a single distribution which is used as an initial set of beam weights for a forward calculation. The results of the forward calculation are inspected for sub-regions of unacceptable overdose and underdose. Adjoint calculations are performed for each such sub-region to better inform the initial set of beam weights. Subsequent forward and adjoint calculations refine the set of beams for the treatment plan. The method was tested with a C-shaped water phantom and with clinical cases. The results indicate that the scheme is able to adjust beam weights effectively and can incorporate different objectives. The method may have the potential to increase the efficiency of the treatment planning process by focusing dose computational resources on the most important elements of the source field. Adjoint calculations are performed with a modified version of MCNP. Forward calculations are performed with MCNPX. An automated script that coordinates adjoint and forward transport is implemented with the MATLAB computing environment.

Key Words: Monte Carlo simulations, inverse treatment planning, IMRT, adjoint transport

INTRODUCTION

The transport of neutral particles through matter is described by the linear form of the Boltzmann transport equation. In radiation therapy, the conventional use of this equation is to transport particles from a source with certain direction and energy characteristics and solve for the distribution of particle flux within a phantom. When this forward flux is coupled to a flux-to-dose conversion factor, (which may be considered an energy-dependent “response function”), the dose deposition may be calculated for a voxel or a region of interest (ROI).

Conversely, the mathematical adjoint to the Boltzmann equation describes the propagation of “adjoint particles” from a voxel with a given energy-dependent response function. This “reverse” transport yields the spatial, angular, and energy distribution of adjoint particles at all locations where a therapy source may be positioned. When this adjoint flux is coupled with the direction and energy characteristics of a source (e.g. an arbitrary set of beams and beam

weights), the dose may be calculated for the voxel (or ROI) that emitted the adjoint particles.¹ Further, this adjoint distribution may be interpreted as an “importance function” because it shows the importance of each source position, direction, and energy to the dose within the voxel.² In this work, we make repeated use of importance functions for tissue ROIs to automatically determine source positions, beam directions, and beam weights for IMRT.

The idea of exploiting adjoint methods for external beam treatment planning is not new. Related work has been published by Gokhale, *et al.*³, Difilippo⁴, Bogner, *et al.*⁵, Jeraj⁶, Jeraj and Keall⁷, and by Yoo, *et al.*⁸ This work differs from previous work by either scale of problem, type of application, or by method of implementation.

Gokhale, *et al.*, compared two adjoint analytic approaches for determining the “path of least resistance” to radiation from the tumor site to the surface of the patient. The flux distribution at the patient surface was considered to be “a hierarchical structure for all possible beam orientations in terms of their effectiveness of delivering dose to the tumor.” This information, in turn, was used to select beam orientations in lieu of hand planning by a clinician. For cases where particle scatter was deemed unimportant, a ray-tracing technique was used to determine the shortest distance of travel from the tumor to the patient surface. Otherwise, a discrete ordinates code (DORT) was used in adjoint mode to generate the flux information. With the exception of their definition of an adjoint source, this work appears to be the first to apply a full adjoint treatment to the transport problem for radiotherapy

Bogner, *et al.*, used a recursive Monte Carlo technique to perform a simultaneous dose calculation and intensity-modulated source optimization for a case with a predefined number of beams, beam orientation, and beam quality. In this work, a forward Monte Carlo simulation is started with a fraction of the total number of histories to be used in the calculation. This initial fraction is used to estimate, voxel by voxel, the “origin of contributions to the energy deposition within [that] voxel.” This information is effectively an adjoint analysis, and is used to compute and refine beam weights at the same time that the Monte Carlo simulation of energy deposition is continued.

Jeraj employed an adjoint treatment of particle collisions to determine relative intensities of adjoint-collided particles at source locations about the patient. The source of particles was a hardened version of the spectrum for a LINAC megavoltage x-ray beam. These relative intensities were used as an initial guess for optimization of beam profiles by simulated annealing. Most recently, Yoo *et al.*, have demonstrated the utility of adjoint analysis as a novel basis for the optimization of brachytherapy prostate implants.

MATERIALS AND METHODS

We have developed an iterative scheme of adjoint and forward Monte Carlo transport calculations to automatically select beams and beam weights for IMRT. The iterative scheme begins with an adjoint calculation for each target and sensitive structure ROI. Adjoint calculations were implemented with the Los Alamos code MCNP.^{9,10} Starting locations for adjoint particles were distributed uniformly throughout an ROI. Starting energies were sampled from an energy-dependent flux-to-dose conversion factor for water.¹¹ Adjoint flux was tallied with a modified point detector tally at 19 positions around a circular gantry, and binned into 40 different directions. The point detector positions exactly coincided with positions where a linac source may be located. The direction bins corresponded to 40 different beamlet directions

available at each source position. The geometry for an initial test phantom is shown in Figure 1. The elliptical phantom was 3 mm thick and had major and minor axes of 20 cm and 7 cm, respectively. Voxel dimensions were $0.2 \times 0.2 \times 0.3 \text{ cm}^3$. The width for a beamlet at 100 cm was 0.5 cm. The target ROI is labeled “TU”, while the sensitive structure ROI is labeled “SS”.

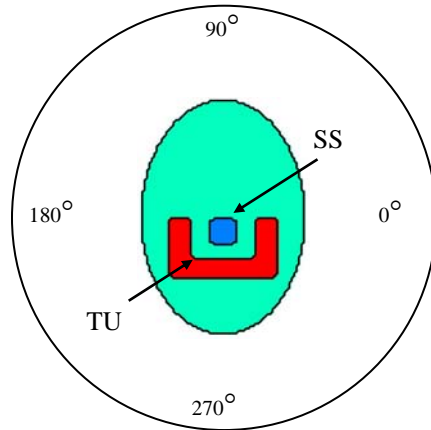


Fig. 1 Phantom, ROI tissue geometry, and circular ‘gantry’ of source positions and adjoint tally locations (4 of 19 are shown).

The adjoint tallies provide an importance function indicating what source positions, and what beamlets are most important to affecting the dose within an ROI. For each direction bin, we combined the adjoint tally for each ROI into a single metric which was then used as the weight for that beamlet in a subsequent forward run. Forward runs were implemented with MCNPX.¹² Dose was scored with a mesh tally with voxel dimensions identical to those in the adjoint case. For the test cases reported here, forward transport was specified as photon only.

For the first iteration of our scheme, (iteration $k=0$), we formed a simple difference between the adjoint tally for the target ROI, Φ_{TU}^+ , and the adjoint tally for the sensitive structure ROI, Φ_{SS}^+ , to form the beam weights for the first forward dose calculation. That is, $w_0 = \Phi_{TU}^+ - \Phi_{SS}^+$, where w_0 signifies the initial set of beam weights, and $w_0 \leftarrow 0$ for $\Phi_{TU}^+ - \Phi_{SS}^+ < 0$. These initial tallies and weights are shown for four source positions in Figure 2.

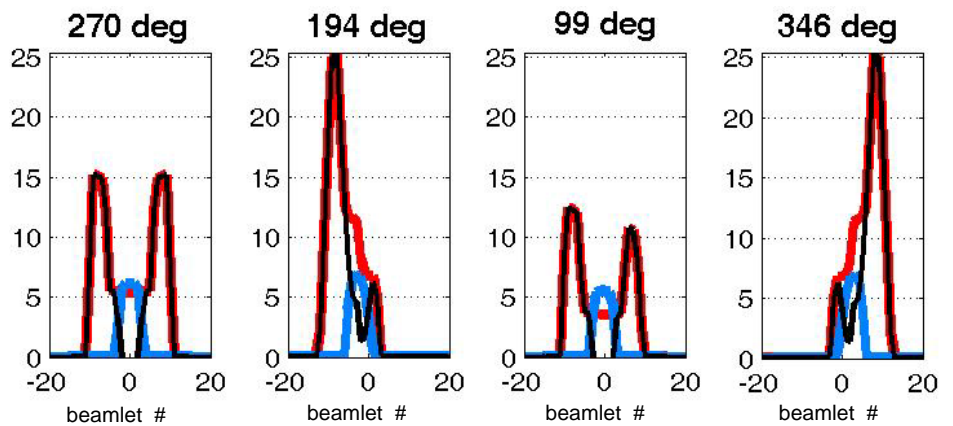


Fig. 2 ROI adjoint tallies and resultant beam weights for four source positions at iteration $k=0$, (arbitrary units)

- TU adjoint tally
- SS adjoint tally
- Initial beam weights

The prescribed dose, D_{PRE} , for the iterative scheme is temporarily set as the average dose from the first forward dose calculation. The ratio between this value and the true prescribed dose level serves as a scaling factor for the final beams weights, so that the true prescribed dose will be delivered. With this definition of D_{PRE} , the next step was to inspect the dose distribution for sub-regions of unacceptable overdose and underdose. For the results presented here, sub-regions for the target ROI were defined simply as any voxels having more than or less than the prescribed dose. For the sensitive structure ROI, overdosed voxels were defined as any voxels having a dose greater than 5% of the prescribed dose. Finally, for normal tissue, overdosed voxels were defined as voxels having greater than 1.05% of the prescribed dose.

Adjoint calculations were performed for each such sub-region to better inform the initial set of beam weights. However, unlike the first adjoint run, the starting location of adjoint particles are not uniformly distributed throughout a sub-ROI. Instead, starting locations are sampled from voxels according to the square of the magnitude of difference between the prescribed dose and a voxel's current dose. Hence, the greater a voxel deviated from the prescribed dose, the greater that voxel was sampled, which led to that voxel having a greater contribution to the adjoint tally and thence a greater weighting (or lesser weighting) for forward beam weights. Iterations of forward and adjoint calculations refine the set of weights for the treatment plan.

RESULTS

The dose distribution after iterations $k=0, 10$, and 40 are shown in Figure 3. For the same iterations, the underdose and overdose regions for the target are shown in Figure 4 and Figure 5, respectively. The quadratic objective function for each iteration is shown in Figure 6. The dose volume histogram for the treatment plan is shown in Figure 7.

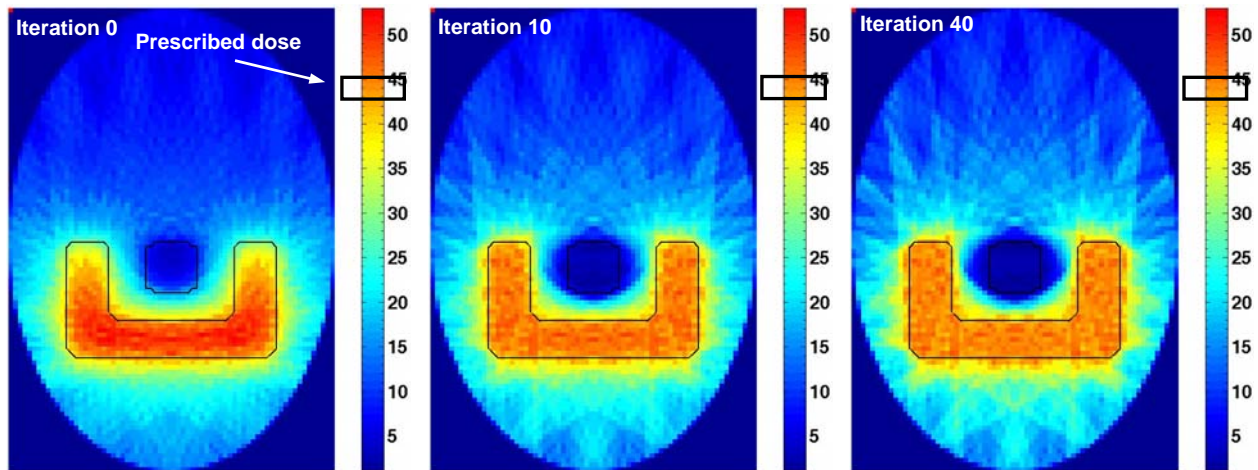


Fig 3. Dose distribution after iterations 0, 10, and 40. Beam weights are updated in each iteration according to the adjoint function of sub-ROI tissue regions that are underdosed or overdosed in the current iteration, (shown in Fig 4 and Fig 5). The adjoint functions for these regions (not shown on this page) are constructed by sampling constituent voxels according to the squared magnitude of their difference from the prescribed dose.

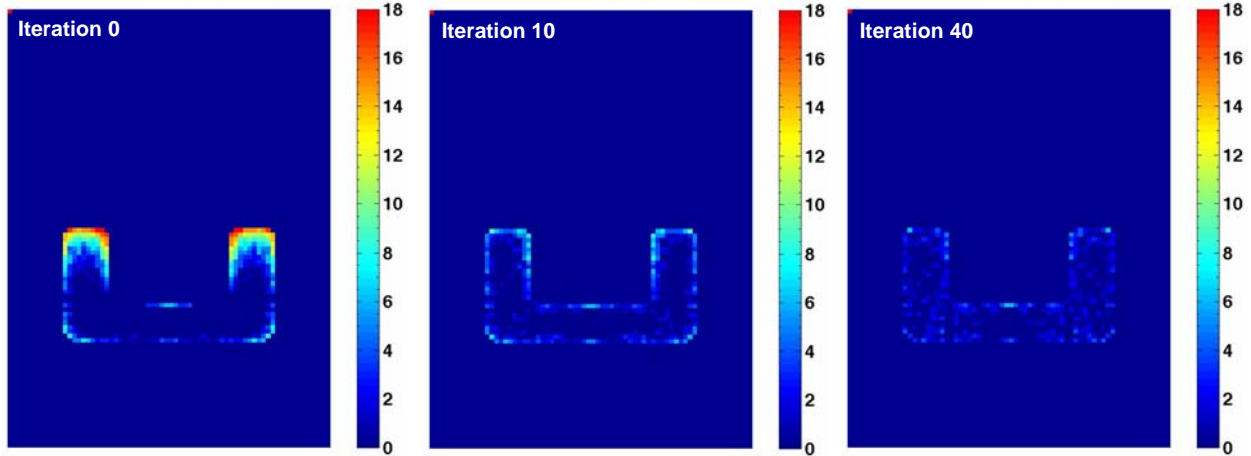


Fig 4. Sub-ROI regions of underdose for iterations 0, 10, and 40. The color in each voxel signifies the difference between the voxel's dose in the current iteration and the prescribed dose. The square of this magnitude is the weight for that voxel's contribution to the sub-ROI adjoint function for updating beam weights for the next iteration.

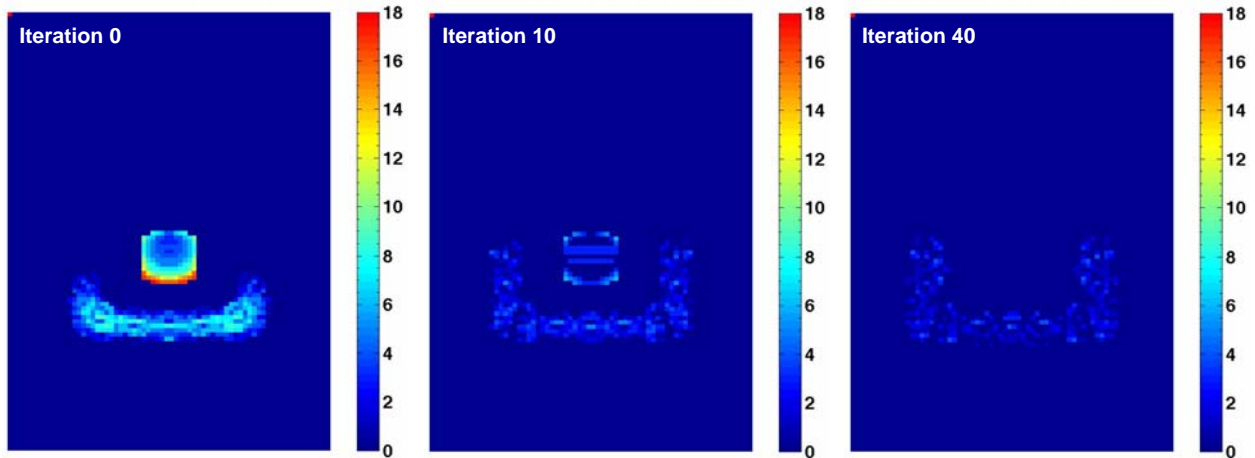


Fig 5. Sub-ROI regions of overdose for iterations 0, 10, and 40. The color in each voxel signifies the difference between the voxel's dose in the current iteration and the prescribed dose. The square of this magnitude is the weight for that voxel's contribution to the sub-ROI adjoint function for updating beam weights for the next iteration.

DISCUSSION

The color of a voxel in Figure 4 and Figure 5 signifies the difference between the prescribed dose and the voxel's dose in the current iteration. The greater this difference, the greater that voxel is sampled in a subsequent adjoint run, which leads to a greater representation in the cumulative adjoint tally, and thence to a refined weighting for forward beam weights. Given that these figures show fewer voxels and smaller magnitudes for later iterations, it appears that the iterative scheme is able to adjust beam weights in an appropriate manner. This trend is also

evident by observing that the magnitude of the total squared difference between the prescribed dose and delivered dose decreases with iteration number (Figure 6).

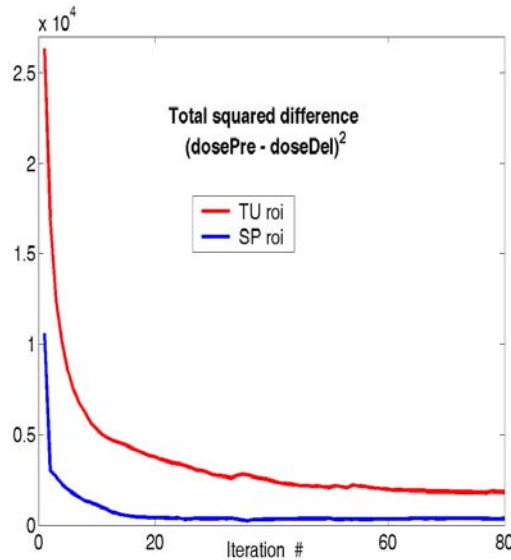


Fig 6. Quadratic objective function score for TU ROI and SS ROI for each iteration.

The dose-volume histogram (DVH) for this result is shown in Figure 7. The DVH for a treatment plan is an evaluation tool that reports the volume of tissue that is raised to a particular dose level. In this case, the iterative scheme has achieved good dose uniformity within the target, with more than 90% of the target receiving 95% of the prescribed dose of 44 Gy.

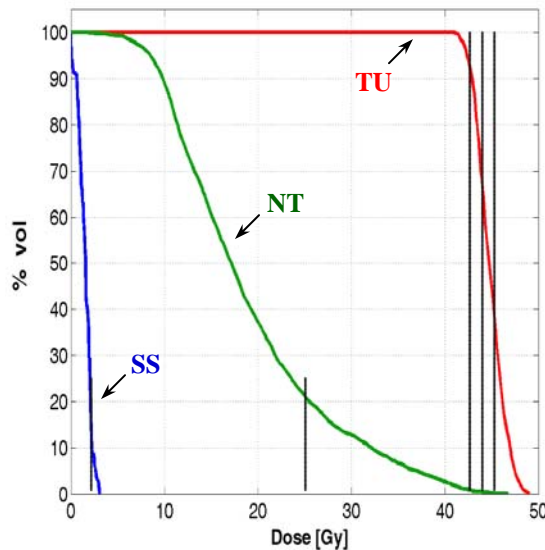


Fig 7. Dose-volume histogram for the result after 80 iterations. The curve labeled “NT” is the DVH for normal tissue.

We are currently examining a variety of means to make this optimization scheme converge more rapidly. However, we believe that this iterative method has the potential to increase the efficiency of the treatment planning process by focusing computational resources on the most important elements of the source field.

CONCLUSIONS

This work examined the use of region-of-interest (ROI) adjoint functions as a tool for developing initial beam weights, and for adjusting the weights of beams that are most important for correcting a residual within the dose field. This iterative method has the potential to increase the efficiency of the treatment planning process by focusing computational resources on the most important elements of the source field.

ACKNOWLEDGMENTS

This work was supported in part by the United States Department of Energy Computational Science Graduate Fellowship (CSGF) Program.

REFERENCES

-
- ¹ E.E. Lewis and W.F. Miller, Jr, *Computational Methods of Neutron Transport*, Wiley, 1993.
 - ² G. I. Bell and S. Glasstone, *Nuclear Reactor Theory*, Krieger Publishing Company, Malabar, FL, 1970.
 - ³ P. Gokhale, E. M. Hussein, and N. Kulkarni, Determination of beam orientation in radiotherapy planning, *Medical Physics*, Volume 21, pp. 393-400, 1994.
 - ⁴ F. Difilippo, Forward and adjoint methods for radiotherapy planning, *Medical Physics*, Volume 25, pp. 1702-1710, 1998.
 - ⁵ L. Bogner, J. Scherer, and M. Herbst, An inverse Monte Carlo optimization algorithm for conformal radiotherapy, *Physica Medica*, Volume 15, 111-119.
 - ⁶ R. Jeraj, *Monte Carlo based inverse treatment planning*, PhD Thesis. University of Ljubljana, 1999.
 - ⁷ R. Jeraj, and P. Keall, Monte Carlo-based inverse treatment planning, *Physics in Medicine and Biology*, 44, 1885-1896.
 - ⁸ S. Yoo, M. E. Kowalok, B. R. Thomadsen, and D. L. Henderson, Treatment planning for prostate brachytherapy using region of interest adjoint functions and a greedy heuristic, *Physics in Medicine and Biology*, Volume 48, pp. 4077-4090.
 - ⁹ J.F. Briesmeister, Editor, *MCNP -- A General Monte Carlo N-Particle Transport Code version 4C*, Technical Report Number LA-13709-M, Los Alamos National Laboratory, Los Alamos, NM, (2000).
 - ¹⁰ J.C. Wagner, J.S. Hendricks, E.L. Redmond, S.P. Palmtag, A. Nagy, and P. Mendius, *MCNP: Multigroup/Adjoint Capabilities*, Technical Report No. LA-12704, Los Alamos National Laboratory, Los Alamos, NM, (1994).
 - ¹¹ American National Standard ANSI/ANS-6.1.1-1977 *Neutron and Gamma-Ray Flux-to-Dose-Rate Factors*, American Nuclear Society, La Grange Park, IL.
 - ¹² J. S. Hendricks, *et al.*, *MCNPX Version 2.5.0*, Technical Report Number LA-UR-04-0570, Los Alamos National Laboratory, Los Alamos, NM, (2004).